Cell Death and Differentiation (2009) 16, 125–138
© 2009 Macmillan Publishers Limited All rights reserved 1350-9047/09 $32.00
www.nature.com/cdd

p47^{phox}-deficient immune microenvironment signals dysregulate naive T-cell apoptosis

M Donaldson[1], A Antignani[2], J Milner[3], N Zhu[1], A Wood[1], L Cardwell-Miller[1], CM Changpriroa[1] and SH Jackson*[,1]

The phagocyte NADPH oxidase is a multicomponent enzyme complex mediating microbial killing. We find that NADPH oxidase p47^{phox}-deficient (p47$^{phox-/-}$) chronic granulomatous disease (CGD) mice develop lymph node hyperplasia even without obvious infection, where increased number of T and B lymphocytes is associated with increased percent of naïve cells and a lower T : B cell ratio than wild type. Paradoxically, despite lymphoid hyperplasia *in vivo*, when lymphocytes are placed in culture, p47$^{phox-/-}$ CD8$^+$ lymphocytes progress more rapidly to apoptosis than wild type. This is associated in cultured p47$^{phox-/-}$ CD8$^+$ lymphocytes with the induction of proapoptotic Bim and Puma expression, increased mitochondrial outer membrane permeabilization and depressed Bcl-2 expression. Addition of IL-7 to the culture partially corrects Bcl-2 levels in cultured p47$^{phox-/-}$ CD8$^+$ lymphocytes and improves the survival. Adding glucose oxidase to the culture to generate hydrogen peroxide along with IL-7 further improves p47$^{phox-/-}$ CD8$^+$ lymphocyte survival, but only to 30% of wild type. We conclude that p47$^{phox-/-}$ CD8$^+$ lymphocytes have an intrinsic survival defect likely in part related to the oxidase deficiency, but *in vivo* in lymph nodes of CGD mice, there are microenvironmental factors yet to be delineated that suppress the progression of apoptosis and allow the accumulation of lymphocytes leading to lymphoid hyperplasia.
Cell Death and Differentiation (2009) **16,** 125–138; doi:10.1038/cdd.2008.129; published online 19 September 2008

Within the complex microarchitecture of secondary lymphoid organs (SLOs), such as lymph nodes (LNs) and spleen, critical signals balance lymphocyte survival and homeostasis. Self-major histocompatibility molecule stimulation of the T-cell receptor (TcR) and extrinsic signals provided by cytokines, such as IL-7 and IL-15 control naïve T-lymphocyte survival.[1,2] In addition, these signals facilitate continuous low-level division of resting naïve T cells during homeostatic proliferation to maintain T-cell number and repertoire diversity.[2] Homeostasis is disrupted during the mounting of an immune response allowing for clonal expansion of effector lymphocytes. Thereafter, the majority of effector cells die to prevent undesirable autoimmunity, and a subset survives as memory T cells.[3,4] Immune responses are mounted within SLOs to eradicate invading pathogens. However, impaired pathogen clearance in an immunocompromised host often results in sustained immune responses that produce local acute inflammatory responses and ultimately systemic chronic inflammation.

Resting naïve T cells recirculate between blood and lymphoid tissues, whereas memory T cells migrate to non-lymphoid tissue sites. Furthermore, without antigen encounter, resting naïve T cells eventually die within a defined half-life.[5,6] Survival of resting naïve T cells during recirculation between inflamed and noninflamed SLOs undoubtedly requires different signals than those required for survival during recirculation between noninflamed SLOs. In this manuscript, we examined the relationship between nicotinamide adenine dinucleotide phosphate (NADPH) oxidase deficiency and naïve T-cell survival within SLOs. The phagocyte multicomponent, NADPH oxidase, mediates the single electron reduction of oxygen to superoxide anion resulting in the well-characterized respiratory burst, which promotes innate cell killing of catalase-positive microorganisms.[7,8] Several nonphagocytic cells have been reported to express ligand-dependent NADPH oxidase-like reactive oxygen species (ROS).[9] We reported that T cells express each of the NADPH oxidase structural proteins and TcR stimulation induces low level intracellular NADPH oxidase-dependent hydrogen peroxide.[10] Chronic granulomatous disease of childhood (CGD) is the genetically inherited primary immunodeficiency, that is caused by defects of structural NADPH oxidase proteins.[11] CGD patients are at increased risk of developing and succumbing to life-threatening infection and acute and chronic inflammatory diseases.[12] Here, we report that NADPH oxidase p47^{phox}-deficient (p47$^{phox-/-}$) mice without the evidence of gross infection develop reactive SLOs characterized by LN hyperplasia with increased B- and T-lymphocyte accumulations.[13] Nearly half of spleen and LN resting p47$^{phox-/-}$ CD8$^+$ lymphocytes rapidly die *ex vivo*, and during the initial 24 h of *in vitro* culture, significantly more resting LN p47$^{phox-/-}$ CD8$^+$ lymphocytes undergo

[1]Monocyte Trafficking Unit, Laboratory of Host Defenses, National Institute of Allergy and Infectious Diseases, National Institutes of Health, Bethesda, MD, USA; [2]Biochemistry Section, Surgical Neurology Branch, National Institute of Neurological Disorders and Stroke, National Institutes of Health, Bethesda, MD, USA and [3]Laboratory of Immunology, National Institute of Allergy and Infectious Diseases, National Institutes of Health, Bethesda, MD, USA
*Corresponding author: SH Jackson, Laboratory of Host Defenses, NIAID, NIH, CRC Building 5-West Labs, Room 5-3942, 10 Center Dr. MSC 1456, Bethesda, MD 20892-1456, USA. Tel: +301 435 8540; Fax: +301 480 3549; E-mail: sjackson@niaid.nih.gov
Keywords: p47^{phox}; T cells; apoptosis; cytokines; apoptosis
Abbreviations: $\Delta\Psi\mu$, mitochondrial transmembrane potential; BrdU, 5-bromo-2′deoxyuridine; CGD, chronic Granulomatous Disease; FSC/SSC, forward and side scatter; GO, glucose oxidase; H_2O_2, hydrogen peroxide; LNs, lymph nodes; MOMP, mitochondrial outer membrane permeabilization; NADPH, nicotinamide adenine dinucleotide phosphate; p47$^{phox-/-}$, oxidase, p47^{phox} deficient; ROS, reactive oxygen species; SLOs, secondary lymphoid organs
Received 17.6.08; revised 25.7.08; accepted 30.7.08; Edited by SJ Martin; published online 19.9.08

caspase-independent cell death than splenic p47$^{phox-/-}$ CD8$^+$ lymphocytes. BH3-only proapoptotic Bim and Puma protein expressions are significantly reduced in LN p47$^{phox-/-}$ CD8$^+$ lymphocytes. However, Bim and Puma expressions are significantly enhanced *in vitro,* and dying p47$^{phox-/-}$ CD8$^+$ lymphocytes from p47$^{phox-/-}$ LNs show increased mitochondrial outer membrane permeabilization (MOMP) and depressed Bcl-2 expression. These results indicate that microenvironmental factors generated during ongoing immune responses in p47$^{phox-/-}$ mice provide signals that regulate naïve T-lymphocyte homeostasis and survival, and may contribute to cellular immune dysfunction in CGD patients.

Results

LN hyperplasia in p47$^{phox-/-}$ mice. p47$^{phox-/-}$ mice have LN hyperplasia, increased total numbers of B and T lymphocytes and lower T : B cell ratios than age- and sex-matched wild-type (WT) mice (Figure 1). However, p47$^{phox-/-}$ and WT CD4 : CD8 ratios were comparable. Flow-cytometry analysis showed p47$^{phox-/-}$ and WT LNs contained phenotypically naïve B220$^+$CD27$^-$ B cells, and comparable phenotypically naïve CD44^{low}CD62L^{high} and CD25^{low}CD69^{low} CD4$^+$ and CD8$^+$ T lymphocytes (Supplementary Figure 1).

In vivo 5-bromo-2′deoxyuridine (BrdU) incorporation studies demonstrated that the peripheral LN CD4$^+$ lymphocyte turnover was similar in p47$^{phox-/-}$ and WT mice, whereas p47$^{phox-/-}$ CD8$^+$ CD44^{high} T cells proliferated 1.5 times more than WT cells (Figure 1c). Peripheral LN p47$^{phox-/-}$ B cells also hyperproliferated compared to WT B cells (Figure 1d). Collectively, these data show that within the reactive p47$^{phox-/-}$ LN microenvironment, there is increased B-cell and memory CD8$^+$-cell divisions along with an increased accumulation of naïve B and T lymphocytes.

Exaggerated death of p47$^{phox-/-}$ CD8$^+$ lymphocytes. Numerous investigations have reported that ROS mediates apoptosis in a variety of cells including T cells. Although investigations of activated T-cell death concluded that excess ROS disrupts mitochondrial membrane integrity by perturbing the balance of Bcl-2 antiapoptotic and proapoptotic proteins, and antioxidants protect activated T cells from ROS-mediated apoptosis,[1,6,14–16] the role of ROS in naïve T-cell survival is less clear. To determine whether NADPH oxidase ROS mediates resting T-cell survival, we examined cytokine responses of LN-derived T lymphocytes. Viable and nonviable lymphocytes from 24 h cultures were differentially stained with DNA-binding dyes and the absolute number of viable *versus* nonviable nucleated cells were quantitated on the basis of cell size and staining properties using the Guava ViaCount assay (see Materials and Methods). Cell count and viability were determined and the data were normalized to the baseline values. After 24 h of culture in IL-2, fewer resting p47$^{phox-/-}$ CD4$^+$ and CD8$^+$ lymphocytes remained viable than WT lymphocytes. Furthermore, there was significantly more cell death of resting p47$^{phox-/-}$ CD8$^+$ lymphocytes (Figure 2).

Both IL-4 and IL-7 have been shown to provide survival signals for resting T cells *in vitro*,[17–21] and studies have shown IL-7 protects resting T cells from apoptotic death by regulating antiapoptotic and proapoptotic Bcl-2 factors.[6,22] Next, we cultured resting p47$^{phox-/-}$ and WT lymphocytes in IL-7 to determine whether IL-7 could rescue dying CD8$^+$ p47$^{phox-/-}$ lymphocytes. At baseline, the percentage of viable p47$^{phox-/-}$ and WT CD8$^+$ cells were comparable. Both WT and p47$^{phox-/-}$ CD8$^+$ lymphocytes cultured in IL-7 for 24 h showed significantly enhanced survival over cells cultured in IMDM alone or with IL-2 (Figure 2b), and p47$^{phox-/-}$ CD8$^+$ lymphocytes cultured in IL-7 contained significantly fewer dead cells than lymphocytes cultured in IL-2 (Figure 2c). However, p47$^{phox-/-}$ CD8$^+$ lymphocytes die at an accelerated rate *in vitro* even when cultured in IL-7, which prevents WT CD8$^+$ cell death.

We previously reported TcR-stimulated T-cell blasts release a prolonged pulse of NADPH oxidase-dependent hydrogen peroxide (H_2O_2).[10] Consequently, to assess whether the survival defect in p47$^{phox-/-}$ CD8$^+$ lymphocytes could be rescued by exogenous H_2O_2, CD8$^+$ cells from p47$^{phox-/-}$ and WT mice were incubated with the H_2O_2 generating enzyme glucose oxidase (GO) for 24 h. GO is a flavoenzyme that catalyses the conversion of β-D-glucose to H_2O_2, and produces a continuous pulse of H_2O_2.[23,24] The combination of GO (1 pg/ml) and IL-7 enhanced p47$^{phox-/-}$-lymphocyte survival 10% over that seen with IL-7 alone (Figure 2d, Supplementary Figure 2). Although 10 ng/ml GO was toxic to p47$^{phox-/-}$ and WT CD8$^+$ cells (data not shown), 1 pg/ml GO was not toxic and did not alter WT-lymphocyte survival. Using lower concentrations of GO (see Materials and Methods) did not improve p47$^{phox-/-}$-lymphocyte survival. These results indicate that exogenous replacement of intracellular H_2O_2 by enzymatic manipulation further enhances IL-7-mediated rescue of p47$^{phox-/-}$ CD8$^+$ lymphocytes.

Prosurvival cytokines IL-2, IL-4, IL-7 and IL-15 are members of the IL-2 family of cytokines that share the common γ-c-receptor subunit,[25] and Park *et al*.[26] showed that these cytokines suppress IL-7 receptor (IL-7R) transcription and expression in resting T cells. To determine p47$^{phox-/-}$ CD8-lymphocyte responsiveness to extrinsic cytokine stimulation, we examined cytokine-regulated IL-7R expression. Freshly isolated resting WT and p47$^{phox-/-}$ cells express comparable levels of surface IL-7R. Similarly, viable WT and p47$^{phox-/-}$ cells downregulated IL-7R after overnight culture in IL-7, but retain surface IL-7R after overnight culture in IL-2 (Supplementary Figure 3). Collectively, these data indicate that although cytokine-activated p47$^{phox-/-}$ CD8$^+$ lymphocytes undergo an exaggerated postactivation cell death *in vitro*, IL-2- and IL-7-triggered common γ-c-receptor pathways in p47$^{phox-/-}$ cells are responsive. In addition, the enhanced rescue of p47$^{phox-/-}$ CD8$^+$ lymphocytes by the combination of IL-7 and GO suggests that NADPH oxidase p47^{phox} and/or NADPH oxidase-mediated ROS may have a preferential role in regulating CD8$^+$-lymphocyte survival.

Resting naïve p47$^{phox-/-}$ CD8 lymphocytes undergo a rapid and profound apoptotic death. To clarify the basis for the exaggerated p47$^{phox-/-}$ CD8$^+$ cell death, we used flow cytometry to assess directly whether there was a

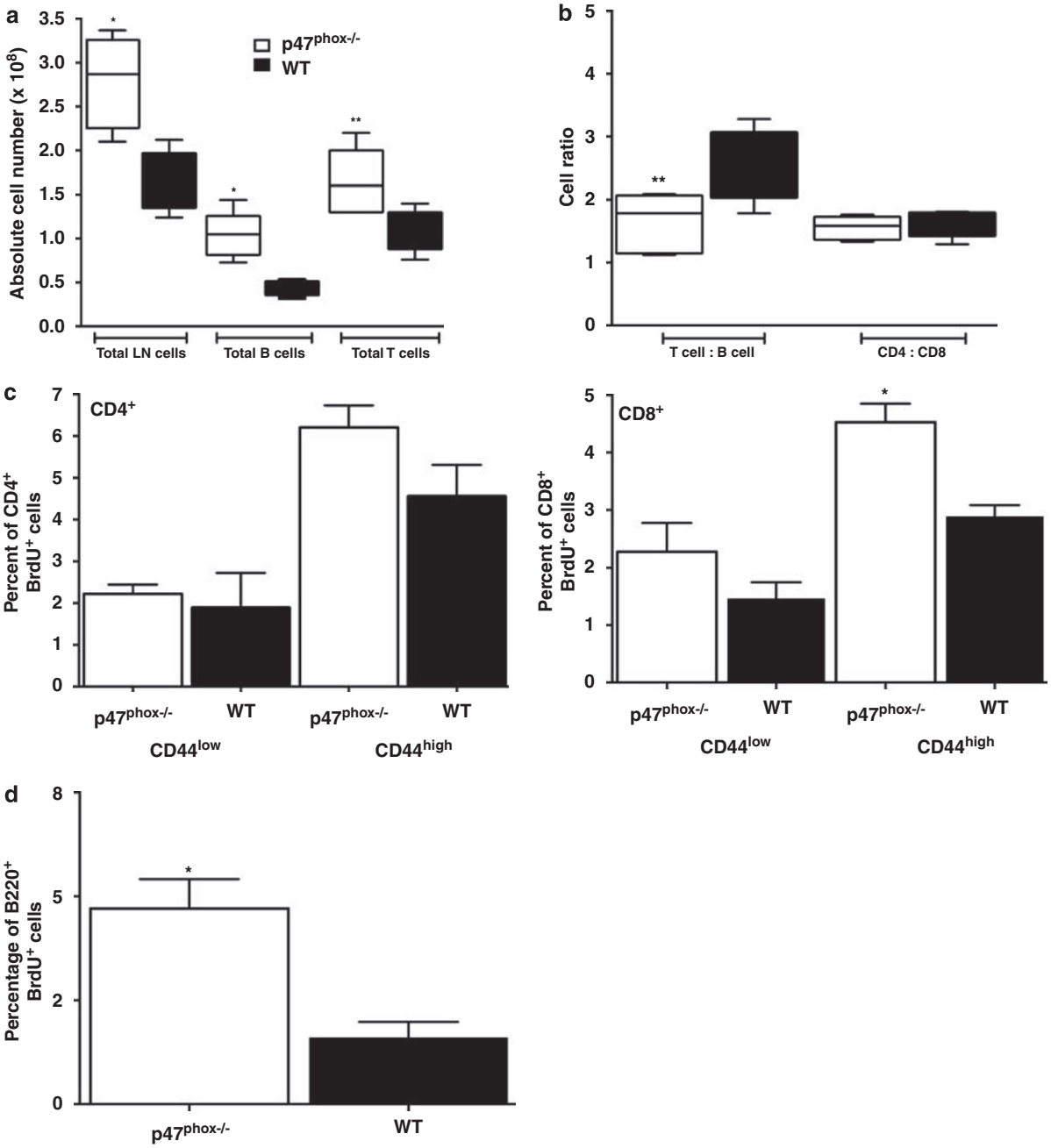

Figure 1 LN hyperplasia *and in vivo* lymphocyte proliferation in p47$^{phox-/-}$ mice. Single cell suspensions of resting LN cells from WT and p47$^{phox-/-}$ mice were generated. Surface B220, CD3 CD8 and CD4 expressions on peripheral LN cells of WT and p47$^{phox-/-}$ mice were assessed by flow cytometry. (**a**) The total number of cells as well as absolute number of B and T lymphocytes isolated from the peripheral LNs of WT and p47$^{phox-/-}$ mice were quantitated. (**b**) The ratios of T : B cells and CD4 : CD8 T cells in the peripheral LNs of WT and p47$^{phox-/-}$ mice were quantitated. The data shown are the mean ± S.E.M. of five independent experiments with three mice/experiment. p47$^{phox-/-}$ responses are indicated by the open histograms and WT responses are indicated by the shaded histograms. *$P = 0.014$, **$P = 0.007$. p47$^{phox-/-}$ and WT mice ($n = 3$) were fed with BrdU in their drinking water at a concentration of 1 mg/ml for 5 days. Lymph nodes were harvested on day 5. Whole lymph node cell populations were stained with anti-CD4, CD8, CD44, B220 and BrdU antibodies and assessed by flow cytometry. (**c**) The percentage of CD44$^{+\,low}$ and CD44^{high} -BrdU$^+$ CD4 (left) and CD8 (right) lymphocytes in WT or p47$^{phox-/-}$ lymph nodes is shown. (**d**) The percent of B220$^+$-BrdU$^+$ lymphocytes in WT or p47$^{phox-/-}$ lymph nodes is shown. *$P < 0.02$

difference in p47$^{phox-/-}$ CD8$^+$-lymphocyte apoptosis. The forward and side scatter (FSC/SSC) properties of p47$^{phox-/-}$ cells cultured with IL-2 or IL-7 for 4 h (Figure 3) and 24 h (data not shown) showed significantly fewer p47$^{phox-/-}$ than WT CD8$^+$ cells were viable, and that the majority of the cells outside of the viable gate were in late apoptosis (Annexin$^+$, 7AAD$^+$). Among the cells in the viable gate (solid line arrows), nearly twice as many p47$^{phox-/-}$ as WT cells cultured in IL-2 were in early (Annexin$^+$, 7AAD$^-$) and late (Annexin$^+$, 7AAD$^+$) apoptosis. For cells cultured in IL-7, twice as many p47$^{phox-/-}$

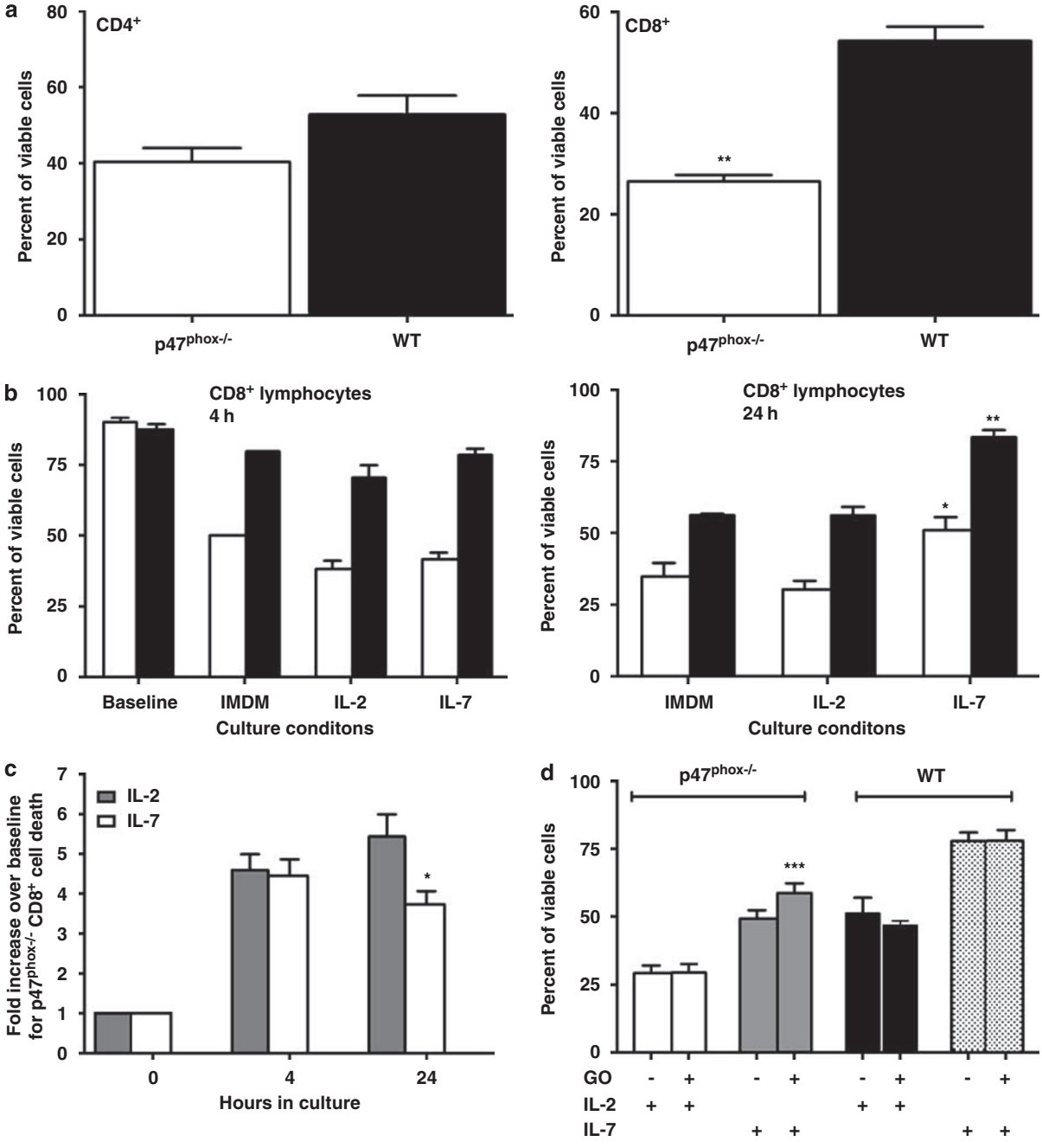

Figure 2 *In vitro* cytokine-activated lymphocyte survival. Fractionated CD4$^+$ and CD8$^+$ p47$^{phox-/-}$and WT lymphocytes were cultured in IMDM alone or supplemented with IL-2 or IL-7, as indicated, for 24 h. The total number of viable and nonviable nucleated cells was measured using the Guava ViaCount assay. p47$^{phox-/-}$ responses are indicated by the open histograms and WT responses are indicated by the shaded histograms. (**a**) The percentage of viable CD4$^+$ (right) and CD8$^+$ (left) p47$^{phox-/-}$ and WT lymphocytes after 24 h in culture. (**b**) The total number of viable and nonviable nucleated CD8$^+$ cells was measured using the Guava ViaCount assay, and responses were normalized to the baseline values. The percentage of viable p47$^{phox-/-}$ and WT cells was quantitated at 4 h (left) and 24 h (right). (**c**) The fold increase in dead CD8$^+$-lymphocyte cell number in the p47$^{phox-/-}$ cultures supplemented with IL-2 (open histogram) and IL-7 (hatched histogram) at 24 h was quantitated. (**d**) Glucose oxidase-produced H_2O_2 enhances p47$^{phox-/-}$ CD8$^+$-lymphocyte survival. Fractionated CD8$^+$ p47$^{phox-/-}$and WT lymphocytes were cultured with IL-2 or IL-7 supplemented culture medium with 1 pg/ml of glucose oxidase (GO) for 24 h. The histograms show the percentage of viable cells at 24 h. p47$^{phox-/-}$ IL-2 ± GO (open histogram), p47$^{phox-/-}$ IL-7 ± GO (gray shaded histogram), WT IL-2 ± GO (black shaded histogram) and WT IL-7 ± GO (hatched histogram). The data shown are the mean ± S.E.M. of four independent experiments with three mice/experiment. *$P = 0.01$, **$P < 0.0001$, ***$P = 0.003$

as WT cells were in late apoptosis. Consistent with the viability data in Figure 2, p47$^{phox-/-}$ viable : late apoptotic cell ratios at 4 *versus* 24 h revealed more p47$^{phox-/-}$ cells continue to die in IL-2 than in IL-7 (1.4 ± 0.07 *versus* 0.44 ± 0.16 $P = 0.02$ for IL-2, and 1.5 ± 0.13 *versus* 1 ± 0.21 for IL-7).

We also activated p47$^{phox-/-}$ and WT CD8$^+$ lymphocytes in the presence of the soluble pan-caspase inhibitor

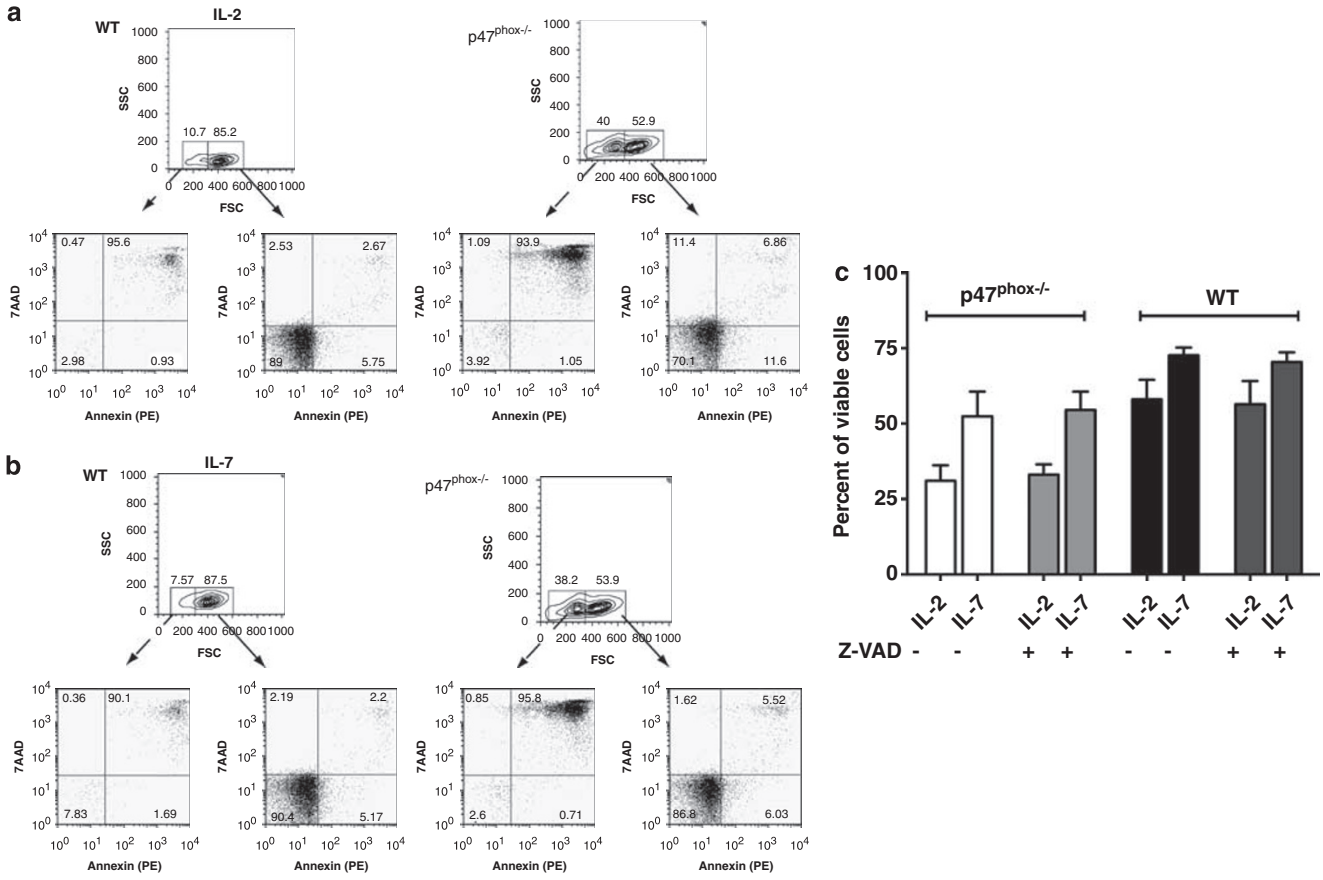

Figure 3 Apoptosis of cytokine-activated CD8$^+$ lymphocytes. Fractionated CD8$^+$ cells were cultured in IMDM supplemented with IL-2 or IL-7. At 3 h, cells were removed from the cultures, stained for surface CD8 and Annexin (X-axis) and 7AAD (Y-axis), and assessed by flow cytometry. The dot plots are gated on the CD8$^+$-cell population. The dot plots show the WT (left) and p47$^{phox-/-}$ (right) Annexin (X-axis) *versus* 7AAD (Y-axis) staining for cells cultured in IL-2 (**a**) or Il-7 (**b**). One representative experiment of four is shown. The data show the responses of 3 – 4 mice/experiment. (**c**) Fractionated CD8$^+$ p47$^{phox-/-}$and WT lymphocytes were cultured in IMDM supplemented with IL-2 or IL-7, with Z-VAD, as indicated, for 24 h. The total number of viable and nonviable nucleated CD8$^+$ cells was measured using the Guava ViaCount assay, and responses were normalized to the baseline values. The percentage of viable p47$^{phox-/-}$ and WT cells at 24 h (right) is shown. The data shown are the mean ± S.E.M. of four independent experiments with three mice/experiment

Z-VAD-FMK, and found there was no difference in the survival of p47$^{phox-/-}$ CD8$^+$ lymphocytes after 24 h (Figure 3c). Collectively, this data indicates that p47$^{phox-/-}$ CD8$^+$ lymphocytes undergo a rapid and profound apoptosis, and the exaggerated *in vitro* p47$^{phox-/-}$ CD8$^+$-lymphocyte cell death is triggered the upstream of caspase-mediated phenomenon.

Impaired survival of p47$^{phox-/-}$ CD8$^+$ cells is due to an intrinsic apoptotic pathway defect. When purified resting naïve mouse T cells are placed into *in vitro* culture in the absence of required survival signals, intrinsic apoptotic pathways are initiated and T cells die rapidly due to the loss of control of mitochondrial homeostasis.[27,28] We cultured resting CD8$^+$ lymphocytes from WT and p47$^{phox-/-}$ mice as described and examined antiapoptotic Bcl-2 and proapoptotic Bax protein expression along with mitochondrial transmembrane potential ($\Delta\Psi$m) and apoptosis to determine whether the exaggerated p47$^{phox-/-}$ CD8$^+$-lymphocyte apoptosis was due to aberrant intrinsic apoptotic pathway function. For these investigations, we performed a multiparametric vitality and apoptosis study using the cyanine dye 1,1′,3,3,3′,3′-hexamethylindodicarbo-cyanine iodide (DiIc$_1$(5)) to assess $\Delta\Psi$m in combination with Annexin-V and 7-AAD to asses apoptosis. In addition, we used surface staining for CD44 to distinguish survival parameters of naïve (CD44^{low}) *versus* activated (CD44^{high}) CD8$^+$ cells. Consistent with the apoptosis data in Figure 2, FSC/SSC properties of p47$^{phox-/-}$ cells after 3 – 4 h of culture showed appreciably fewer p47$^{phox-/-}$ CD8 cells were viable (Figure 4). Additionally, as shown in histogram overlays of WT (bold-lined histograms) and p47$^{phox-/-}$ (shaded histograms) CD8$^+$ lymphocytes, we also observed a dramatic and rapid shift of the p47$^{phox-/-}$ CD8$^+$-lymphocyte CD44 profile. Although the baseline CD44 WT and p47$^{phox-/-}$ CD8$^+$-lymphocyte profiles were essentially identical, after just 3 h in culture approximately 1/3 of p47$^{phox-/-}$ CD8$^+$ cells are CD44^{high} suggesting that during *in vitro* culture there is a preferential loss of naive CD44^{low} p47$^{phox-/-}$ CD8$^+$ lymphocytes. Further, after 24 h, we found that among the remaining viable p47$^{phox-/-}$ CD8$^+$ lymphocytes, the majority of cells were CD44$^{moderate\text{-}to\text{-}high}$ in each of the culture conditions.

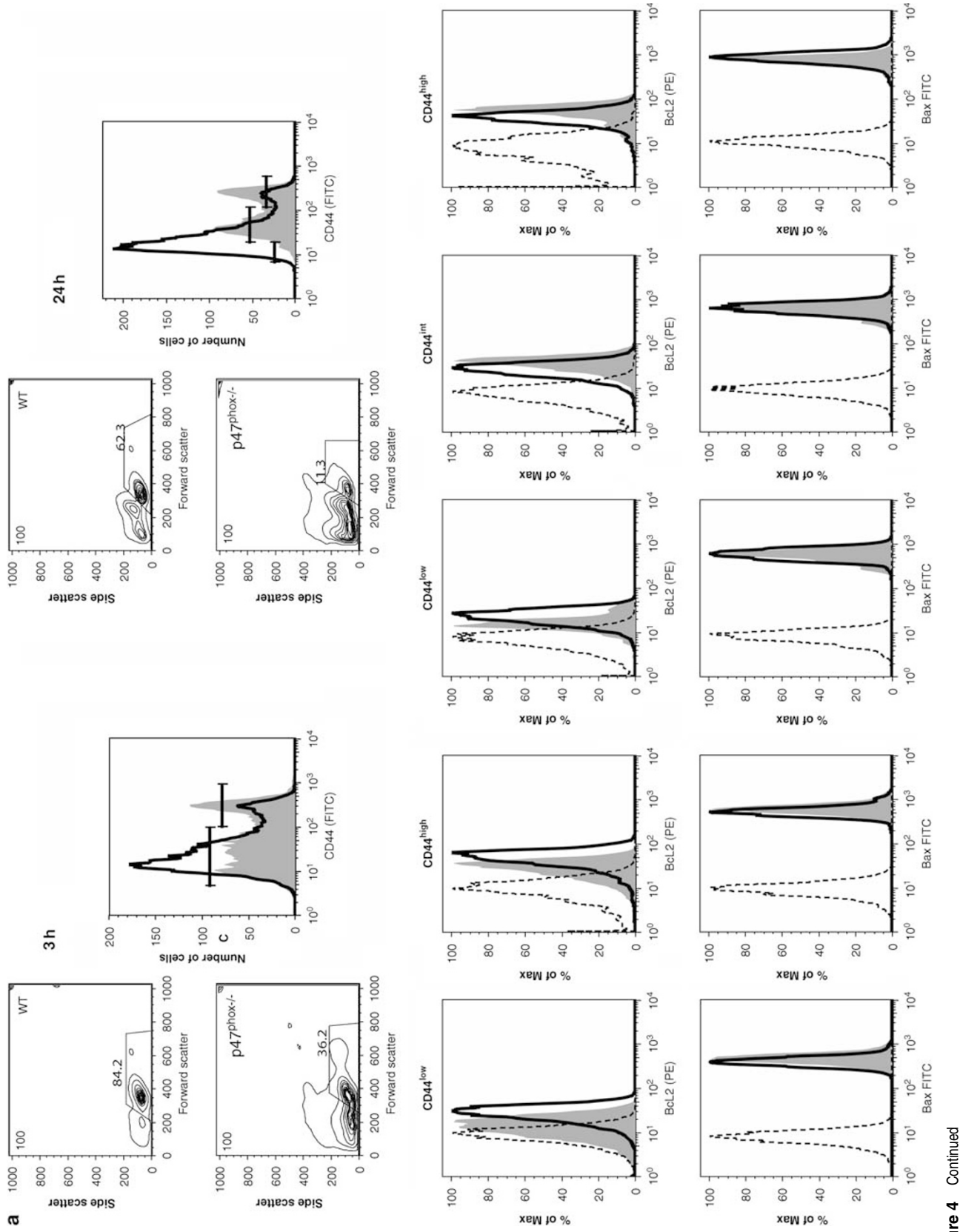

Figure 4 Continued

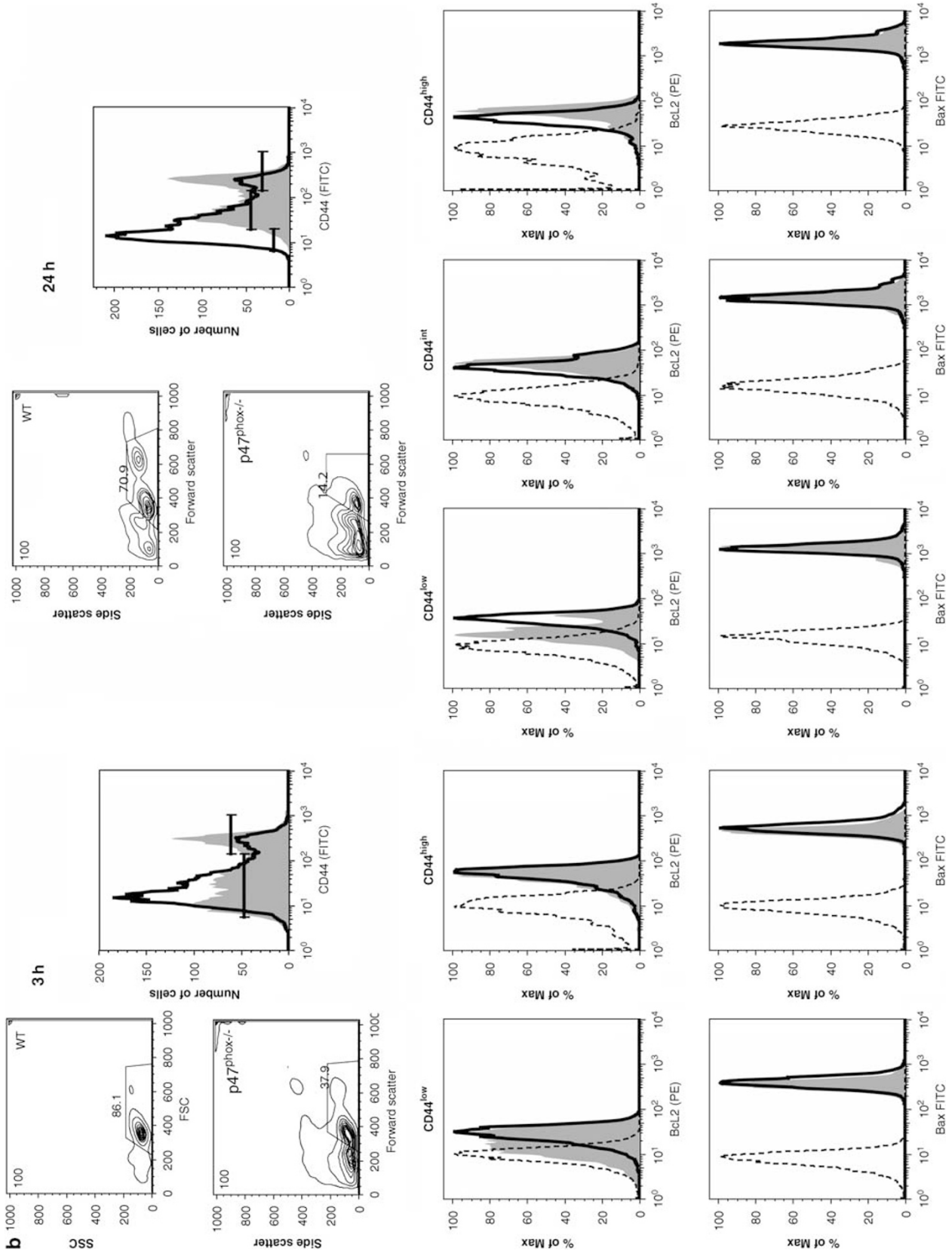

Figure 4 Continued

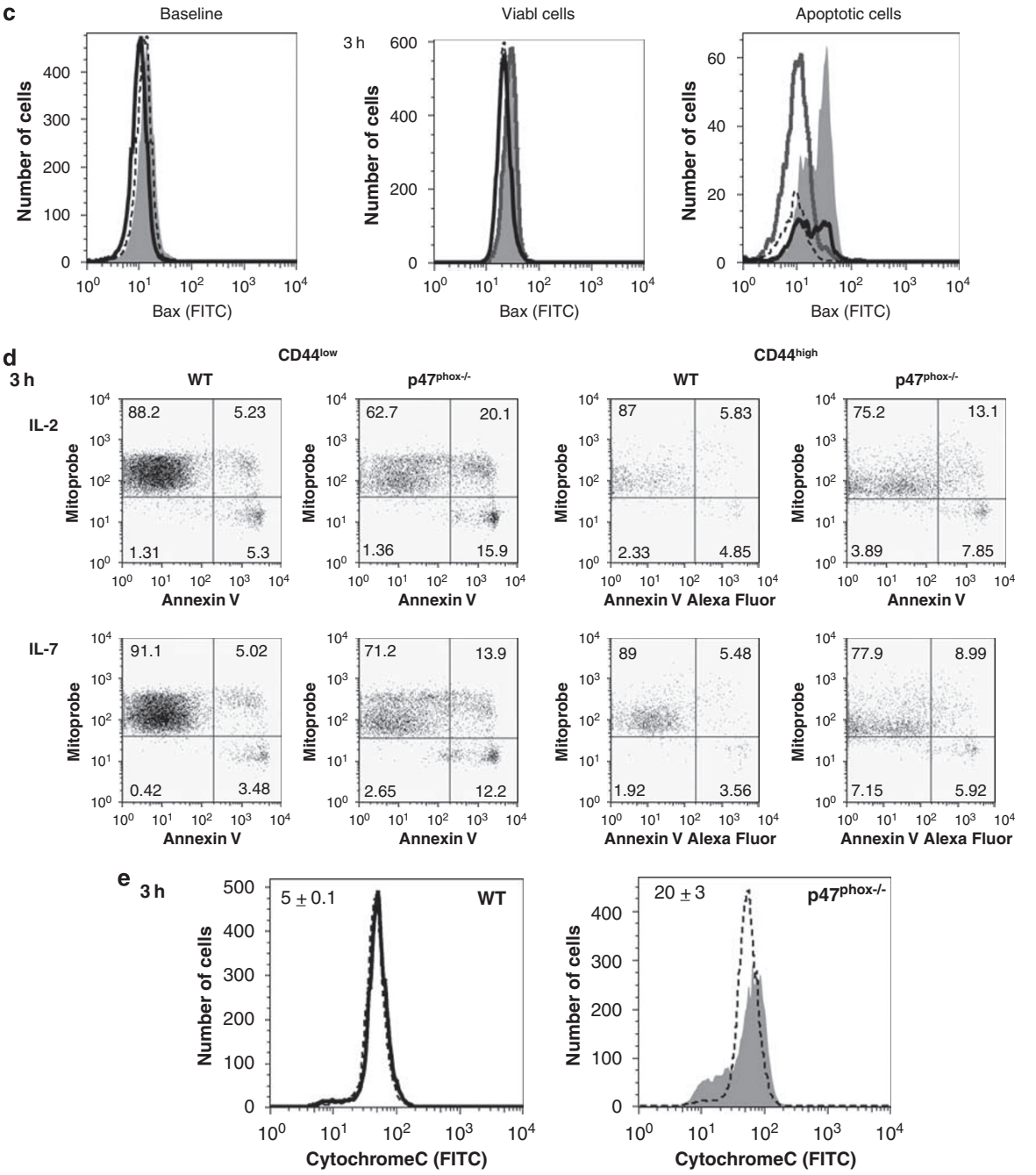

Figure 4 Intrinsic apoptotic pathway defect in cytokine-activated p47$^{phox-/-}$ CD8$^+$ lymphocytes. Fractionated CD8$^+$ p47$^{phox-/-}$ and WT lymphocytes were cultured in IMDM supplemented with IL-2 (**a**) or IL-7 (**b**) for 24 h. At 3 h (right) and 24 h (left), cells were removed from the cultures, stained for surface CD8 and CD44, fixed, permeabilized and stained with anti-Bcl-2 or anti-Bax as indicated. The contour plots show the forward scatter *verses* side scatter cell phenotype and the analysis gates. The adjacent histograms show the flow cytometry phenotype of the CD8$^+$CD44$^+$ p47$^{phox-/-}$ (filled tinted histograms) and WT (bold-lined histograms) cells. The gates on the CD44 histograms correspond to the CD44^{low}, CD44^{intermediate} and CD44^{high} populations used to generate the histograms showing the anti-Bcl-2 or anti-Bax staining for p47$^{phox-/-}$ (shaded histograms) and WT (bold-lined histograms) cells and the isotype control staining for p47$^{phox-/-}$(dot-lined histogram) and WT (dash-lined histogram) cells. One representative experiment of three is shown. The data shows the responses of three mice/experiment. (**c**) Proapoptotic conformational change in Bax. Fractionated CD8$^+$ p47$^{phox-/-}$ and WT lymphocytes were cultured in IMDM supplemented with IL-2 for 3 h, and then fixed, permeabilized and stained with conformation-specific anti-Bax (6A7) antibody as indicated. One representative experiment of two is shown. (**d**) Fractionated CD8$^+$ p47$^{phox-/-}$ and WT lymphocytes were cultured in IMDM supplemented with IL-2 or IL-7 as indicated. At 3 h, cells were removed from the cultures, stained for surface CD8 and CD44, Annexin, PI and mitoprobe. The dot plots are gated on the CD8$^+$-cell population. The dot plots show the CD44^{low} (left) *versus* CD44^{high} (right) populations of WT and p47$^{phox-/-}$ mitoprobe (Y-axis) *versus* PI (X-axis) and mitoprobe (Y-axis) *versus* Annexin (X-axis) staining for cells cultured in IL-2 or Il-7 as indicated. One representative experiment of three is shown. (**e**) CytochromeC release in p47$^{phox-/-}$ CD8$^+$ lymphocytes at baseline (dash-lined histograms) and 3 h (WT: bold-lined histogram, p47$^{phox-/-}$: shaded histogram) of culture with IL-2 as indicated. Fractionated CD8$^+$ p47$^{phox-/-}$ and WT lymphocytes were cultured in IMDM supplemented with IL-2 for 3 h, and then permeabilized with digitonin, fixed, immunostained with an anticytochromeC antibody. One representative experiment of three is shown. Numbers indicate percentage of cells (mean ± S.E.M.) with low fluorescence (cytochromeC release) for the three replicates. The data show the responses of 3–4 mice/experiment

Baseline Bcl-2 expression for WT and p47$^{phox-/-}$ CD8$^+$ cells were essentially identical (Supplementary Figure 4), however, Bcl-2 expression was rapidly and dramatically reduced in CD44^{low} and CD44^{high} p47$^{phox-/-}$ CD8$^+$ lymphocytes compared to WT lymphocytes cultured in IL-2 for 3 h (Figure 4a). After 24 h, Bcl-2 expression in CD44^{moderate} and CD44^{high} p47$^{phox-/-}$ cells was comparable to WT CD8$^+$ lymphocytes. For cells cultured in IL-7 (Figure 4b), we found that Bcl-2 was rapidly and dramatically reduced in CD44^{low} p47$^{phox-/-}$ CD8$^+$ lymphocytes compared to WT CD8$^+$ lymphocytes after 3 h. However, Bcl-2 was comparable in WT and p47$^{phox-/-}$ CD44^{high} CD8$^+$ lymphocytes at 3 h. After 24 h, we found a small fraction of CD44^{low} p47$^{phox-/-}$ cells cultured with IL-7 retained Bcl-2, and as with IL-2 cultured cells, Bcl-2 expression in CD44^{moderate} and CD44^{high} p47$^{phox-/-}$ cells was comparable to WT. Bax expression in p47$^{phox-/-}$ CD8$^+$ lymphocytes was comparable to WT lymphocytes cultured in IL-2 and in IL-7 for each characterized CD44 population. Additionally, Bax undergoes proapoptotic conformational changes in both WT and p47$^{phox-/-}$ apoptotic CD8$^+$ lymphocytes (Figure 4c). These results indicate that the rapid loss of Bcl-2, preferentially among naïve CD44^{low} cells, contributes to the profound death of p47$^{phox-/-}$ CD8$^+$ lymphocytes *in vitro*. Furthermore, the ability of IL-7 to partially rescue p47$^{phox-/-}$ CD8$^+$ lymphocytes from an exaggerated cell death *in vitro* is due in part to its regulation of Bcl-2 protein levels, especially among viable CD44^{high} cells during the initial 3 h of culture.

Finally, when we examined the cells for $\Delta\Psi$m, we observed that as rapidly as 3 h fewer CD44^{low} and CD44^{high} p47$^{phox-/-}$ CD8$^+$ lymphocytes than WT retained the cyanine iodide dye (MtP$^+$Ann$^-$), indicating significantly more MOMP (Figure 4d, Table 1).[27] We also found that compared to IL-7 cultured cells, significantly more CD44^{low} p47$^{phox-/-}$ lymphocytes cultured with IL-2 showed reduced $\Delta\Psi$m (Table 1). In additional experiments we confirmed that in addition to the loss of $\Delta\Psi$m, dying p47$^{phox-/-}$ CD8$^+$ lymphocytes also release mitochondrial cytochrome C (Figure 4e). For these analyses, we used a quantitative flow cytometric assay to differentiate cells with intact mitochondria (high fluorescence) from cells that had released mitochondrial cytochrome C (low fluorescence).[29,30] As indicated in the histograms in Figure 4e, the majority of WT lymphocytes had intact mitochondria at baseline and after culture in IL-2. However, although the majority of p47$^{phox-/-}$ lymphocytes also had intact mitochondria at baseline after 3 h in culture, cytochrome C was released in the apoptotic p47$^{phox-/-}$ cells (21% ± 3 p47$^{phox-/-}$ *versus* 5 ± 0.1 WT, $P = 0.005$). Collectively, these observations implicate a role for NADPH oxidase p47^{phox} as an upstream effector of the mitochondrial apoptosis pathway via regulation of the antiapoptotic protein Bcl-2.

Survival of p47$^{phox-/-}$ CD8$^+$ cells is dependent upon the lymphoid microenvironment. T-lymphocyte homeostasis is tightly controlled by multiple regulatory checkpoints that restrain T-lymphocyte differentiation within the thymus and expansion in the periphery. Post-thymic export resting naïve T cells are found concentrated in SLOs. However, resting naïve T cells are not stationary but constantly traffic between SLOs in search of antigen, thus providing an effective surveillance system within lymphoid organs. We compared survival of thymic, spleen and LN-derived resting naïve p47$^{phox-/-}$ CD8$^+$ lymphocytes to discern whether the observed survival defect could be linked to the NADPH oxidase p47$^{phox-/-}$ physiologic microenvironment (Figure 5). We found that single positive p47$^{phox-/-}$ CD8$^+$ thymocytes survived as well as WT thymocytes, whereas significantly more splenic resting p47$^{phox-/-}$ CD8$^+$ lymphocytes rapidly succumb during the initial 3–4 h of *in vitro* culture in IL-2 or IL-7 similar to LN (Figure 2) p47$^{phox-/-}$ CD8$^+$ lymphocytes. However, unlike LN p47$^{phox-/-}$ CD8$^+$ lymphocytes, the majority of the remaining splenic p47$^{phox-/-}$ CD8$^+$ lymphocytes remained viable after 24 h of culture in IL-2 or IL-7. Additionally, there was no difference in the *in vitro* survival of splenic p47$^{phox-/-}$ CD8$^+$ lymphocytes cultured with IL-2 or IL-7 after 24 h. Consequently, post-thymic survival of resting naïve p47$^{phox-/-}$ CD8$^+$ lymphocytes is highly variable and significantly impacted by NADPH oxidase p47$^{phox-/-}$ SLO microenvironmental factors.

Although WT and p47$^{phox-/-}$ LN CD8$^+$ lymphocytes have comparable baseline Bcl-2 and Bax expression, Bcl-2 rapidly declines in p47$^{phox-/-}$ CD8$^+$ lymphocytes *in vitro,* while Bax remains stable. We also found that antiapoptotic Mcl-1 expression was comparable in resting naïve WT and p47$^{phox-/-}$ LN CD8$^+$ lymphocytes at baseline and after *in vitro* culture (data not shown). The observed dysregulation of the intrinsic pathway *in vitro* lead us to question whether BH3-only proteins that regulate Bcl-2[31] are aberrant in p47$^{phox-/-}$ CD8$^+$ lymphocytes. We found that baseline Puma and Bim EL expressions were significantly reduced in LN p47$^{phox-/-}$ CD8$^+$ lymphocytes compared to WT lymphocytes. However, after 2 h of *in vitro* culture, LN p47$^{phox-/-}$ CD8$^+$ lymphocytes expressed significantly more Bim EL and Bim L as well as Puma (Figure 6). For spleen, WT and p47$^{phox-/-}$ CD8$^+$ lymphocytes showed comparable Bim and Puma expressions at baseline (data not shown). However, similar to LN, Bim EL and Puma were significantly induced

Table 1 Mitochondrial outer membrane permeabilization (MOMP) of cytokine-stimulated CD8$^+$ lymphocytes

	CD44^{low}				CD44^{high}			
	Live (MtP$^+$Ann$^-$)		Apoptotic (MtP$^+$Ann$^+$)		Live (MtP$^+$Ann$^-$)		Apoptotic (MtP$^+$Ann$^+$)	
	IL-2	IL-7	IL-2	IL-7	IL-2	IL-7	IL-2	IL-7
p47$^{phox-/-}$	38 ± 14	45 ± 13	46 ± 11	40 ± 11	55 ± 7.7	60 ± 6.7	30 ± 5.8	24 ± 5
Wild type	76 ± 8.6	78 ± 9.7	16 ± 6.8	17 ± 7.5	79 ± 4.5	83 ± 3.5	10 ± 2.6	12 ± 2.7

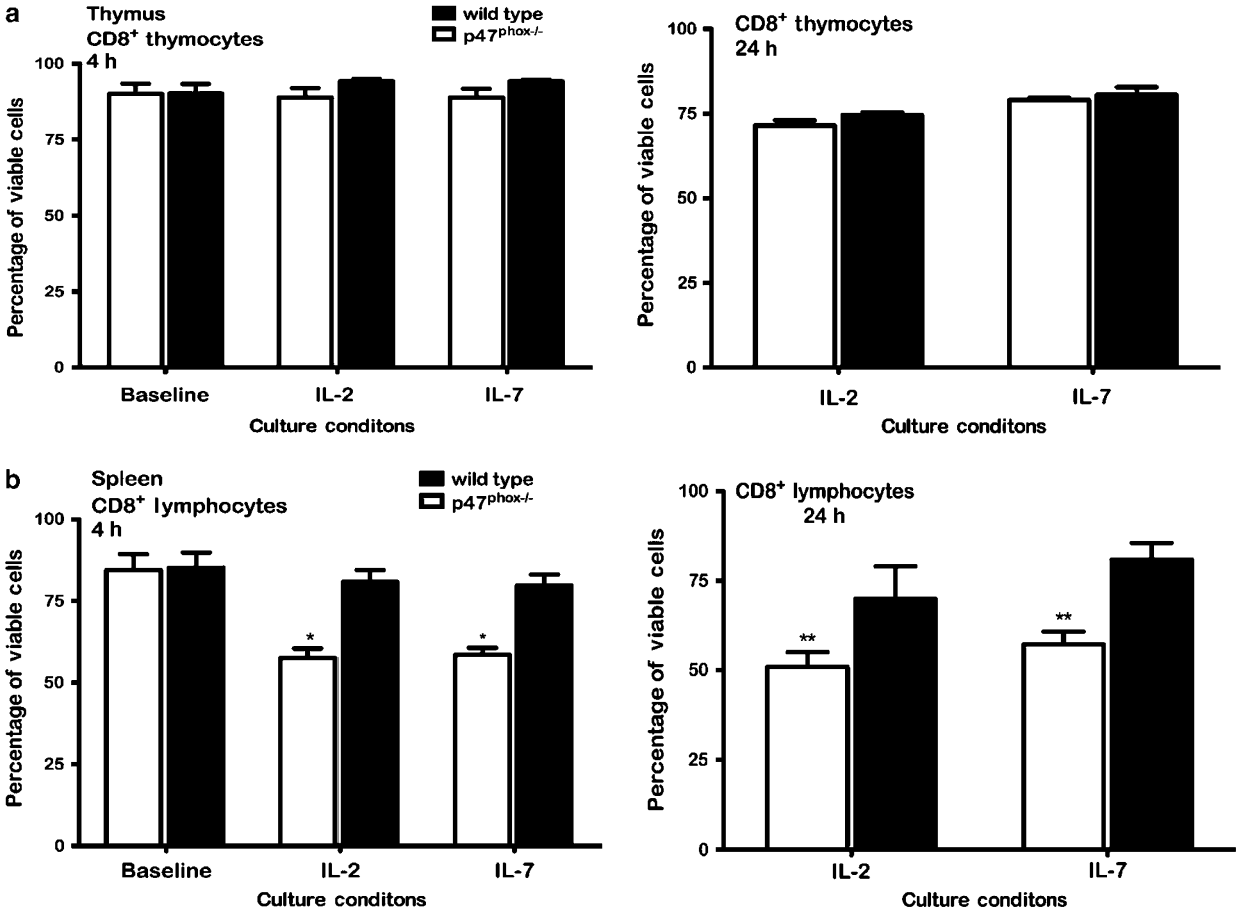

Figure 5 *In vitro* cytokine-activated thymocyte and splenic lymphocyte survival. Fractionated CD8$^+$ p47$^{phox-/-}$and WT single positive thymocytes or splenic lymphocytes were cultured in IMDM supplemented with IL-2 or IL-7 as indicated for 24 h. The total number of viable and nonviable nucleated CD8$^+$ cells was measured using the Guava ViaCount assay, and responses were normalized to the baseline values. p47$^{phox-/-}$ responses are indicated by the open histograms and WT responses are indicated by the shaded histograms. (**a**) The percentage of viable CD8$^+$ p47$^{phox-/-}$ and WT thymocytes at 4 (left) and 24 h (right) in culture. (**b**) The percentage of viable CD8$^+$ splenic p47$^{phox-/-}$ and WT lymphocytes after 4 (left) and 24 h (right) in culture. The data shown are the mean ± S.E.M. of three independent experiments with 3 – 4 mice/experiment. $^*P<0.001$, $^{**}P<0.02$

in vitro in splenic p47$^{phox-/-}$ CD8$^+$ lymphocytes compared to WT (Figure 6). These results suggest that resting naïve p47$^{phox-/-}$ CD8$^+$ within p47$^{phox-/-}$ SLOs are signaled to suppress proapoptotic protein expression.

To assess the fate of p47$^{phox-/-}$ T cells within normal SLO microenvironments, we adoptively transferred equal numbers of resting WT and p47$^{phox-/-}$ splenocytes into a WT recipient. Similar to what we observed *in vitro,* the ratio of p47$^{phox-/-}$: WT lymphocytes recovered from the LNs and spleens of recipient mice 24-h post-adoptive transfer indicates a profound loss of p47$^{phox-/-}$ cells (Figure 7). We also observed a greater loss of p47$^{phox-/-}$ CD8$^+$ cells than CD4$^+$ cells, and found that there was a greater loss of naïve p47$^{phox-/-}$ CD44^{low}CD8$^+$ lymphocytes than CD44^{high} lymphocytes *in vivo*.

In summary, these observations implicate a role for NADPH oxidase p47^{phox} as an upstream effector of the mitochondrial apoptosis pathway via regulation of Bcl-2 protein family members. Furthermore, the increase death of adoptively transferred p47$^{phox-/-}$ CD8$^+$ lymphocytes within WT mouse SLOs suggest that the signals generated within the complex NADPH oxidase p47$^{phox-/-}$ SLO microenvironment restrain CD8$^+$ lymphocyte apoptosis.

Discussion

Previous observations revealed that T cells express each of the NADPH oxidase structural proteins; pg91^{phox} p22^{phox} p47^{phox} and p67^{phox} and TcR stimulation induces low level intracellular NADPH oxidase-dependent H_2O_2.[10] These observations suggested a role of NADPH oxidase-mediated ROS in T-cell function. We report that post-thymic resting naïve p47$^{phox-/-}$ CD8$^+$ cells exhibit an intrinsic survival defect. We link the defect to higher levels of intrinsic apoptotic pathway activity in p47$^{phox-/-}$ CD8$^+$ lymphocytes *in vitro* and showed that naïve CD44^{low} p47$^{phox-/-}$ lymphocytes have lower Bcl-2 levels that are only partially rescued by prosurvival cytokine IL-7. We also found that *in vitro* p47$^{phox-/-}$ CD8$^+$-lymphocyte survival could be distinguished by BH3-only Bim and Puma protein expression. Although Bim and Puma were significantly reduced in isolated LN p47$^{phox-/-}$ CD8$^+$ lymphocytes, protein expression in splenic p47$^{phox-/-}$ CD8$^+$ lymphocytes was comparable to WT lymphocytes. Interestingly, both proteins were induced *in vitro* in LN and splenic p47$^{phox-/-}$ CD8$^+$ lymphocytes indicating that enhanced Bim and Puma expression regulates the rapid *in vitro* death of p47$^{phox-/-}$ cells.

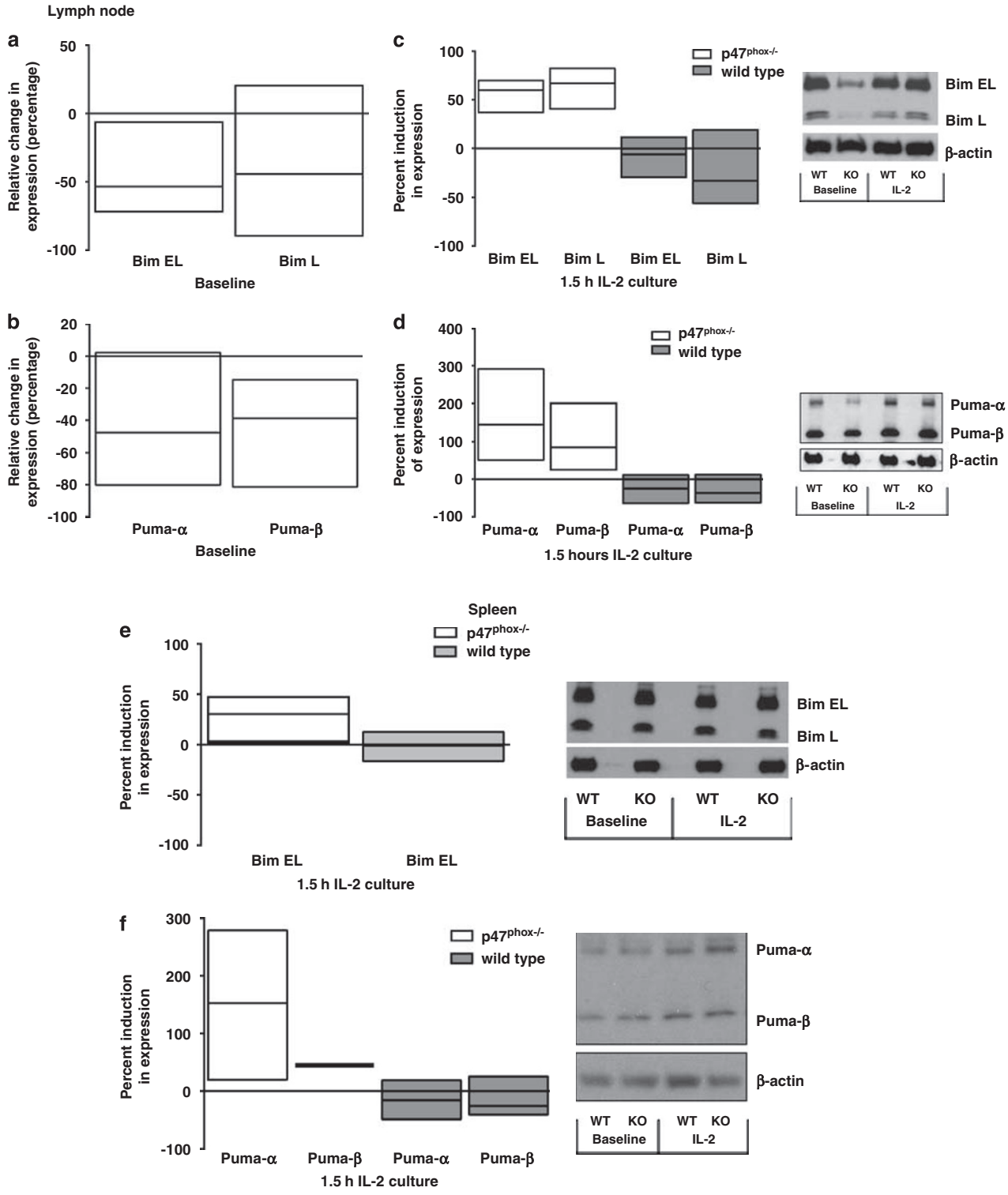

Figure 6 Secondary lymphoid organ factors alter BH3-only Bim and Puma expressions in p47$^{phox-/-}$ CD8$^+$ lymphocytes. Fractionated CD8$^+$ p47$^{phox-/-}$and WT lymphocytes were cultured in IMDM supplemented with IL-2 for 1.5 h. Baseline and 1.5 h western blot analysis for Bim or Puma expressions were performed as described in the Materials and Methods. Bars show the quantitative analysis (mean ± S.E.M.) of lymph node and spleen lymphocyte protein expression. The percent change in LN p47$^{phox-/-}$CD8$^+$ lymphocyte Bim (**a**) or Puma (**b**) expression compared to WT CD8$^+$-lymphocyte protein expression. The percentage induction in Bim (**c**) or Puma (**d**) expressions in lymph node p47$^{phox-/-}$ CD8$^+$ lymphocytes at 1.5 h of culture compared to baseline protein expression. The percentage induction in Bim (**e**) or Puma (**f**) expressions in splenic p47$^{phox-/-}$ CD8$^+$ lymphocytes at 1.5 h of culture compared to baseline protein expression. The data shown are the mean ± S.E.M. of three independent experiments with 3–4 mice/experiment. Representative western blot analysis of Bim or Puma expression in lymph node and spleen are shown adjacent to the bar graphs

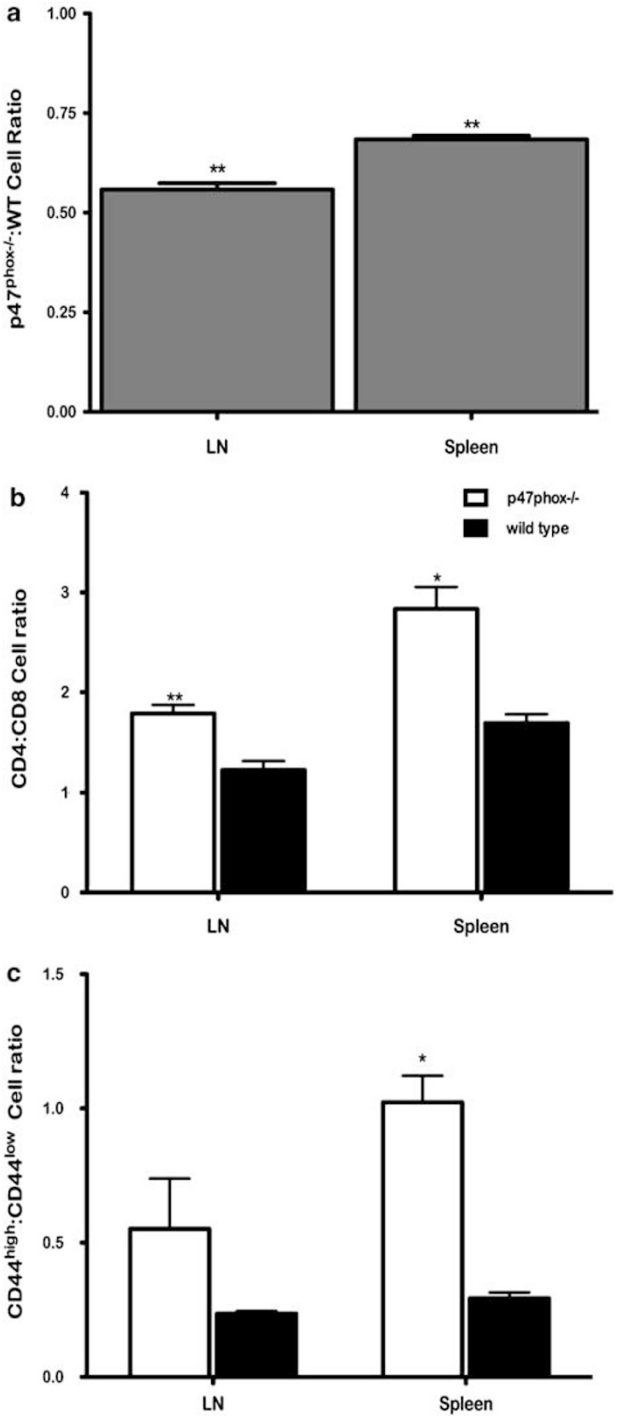

Figure 7 Unrestrained death of p47$^{phox-/-}$ lymphocytes in WT secondary lymphoid organs. Single cell suspensions of resting LN cells from WT and p47$^{phox-/-}$ mice were generated and pooled. A total of 10×10^6 LN cells were transferred into Ly5.1 congenic recipient mice ($n=3$). After 24 h, the recipients were killed, and lymph nodes and spleen were harvested and stained for surface markers. Cells were gated on CD45.2$^+$ CD45.1$^-$, and then analyzed for CD4, CD8 and CD44 staining among WT (Thy1.1$^+$, Thy1.2$^-$) or p47$^{phox-/-}$ (Thy1.2$^+$, Thy1.1$^-$) donor T cells in the (**a**) LNs and (**b**) spleens. The results show the cell ratios for p47$^{phox-/-}$: WT donor cells (gray histogram) and the CD4 : CD8 and CD8$^+$ CD44^{high} : CD44^{low} for p47$^{phox-/-}$ or WT cells as indicated. *$P<0.01$, **$P<0.04$

Supplementing cultures with exogenous IL-7 *in vitro* normally regulates cellular Bcl-2 proteins to maintain equilibrium of antiapoptotic and proapoptotic proteins. However, even with the addition of IL-7 leading to a demonstrative reduction in resting p47$^{phox-/-}$ lymphocyte death after 24 h in culture, the overall survival of p47$^{phox-/-}$ lymphocytes was only 61%, $P<0.0001$, of WT cells. Thus, indicating that additional and as yet defined signaling events may be aberrant in p47$^{phox-/-}$ lymphocytes. On the basis of our observation that NADPH oxidase-dependent H_2O_2 is differentially regulated in activated T-cell blasts,[10] we asked whether the aberrant death of p47$^{phox-/-}$ CD8$^+$ cells was due to H_2O_2 deficiency. To avoid the potential of causing oxidative stress in our *in vitro* culture model,[32] we used GO rather than an H_2O_2 bolus to restore intracellular H_2O_2 in p47$^{phox-/-}$ cells. However, one of the inherent limitations of this *in vitro* experimental design is that we cannot control the timing of H_2O_2 generation. Subsequently, it is unclear whether the partial rescue of p47$^{phox-/-}$ CD8$^+$ cells is due to a disparity in the timing of H_2O_2 delivery. The finding that the optimal survival of p47$^{phox-/-}$ CD8$^+$ cells only occurred when both GO and IL-7 were used indicates neither is sufficient to support resting p47$^{phox-/-}$ CD8$^+$-cell survival. However, finding that low-level H_2O_2 enhances IL-7-mediated p47$^{phox-/-}$ CD8$^+$-cell survival suggests an optimum physiologic H_2O_2 concentration released at the appropriate time during cytokine stimulation maybe a previously unrecognized pivotal, although partial, signal for lymphocyte survival. We plan to examine these questions in future investigations.

Immune responses are mounted within SLOs to eradicate invading pathogens. However, impaired pathogen clearance in immunocompromised host often results in sustained immune responses. Furthermore, the persistent immune challenge experienced by immunocompromised host undermines the need to maintain a consistent level of naïve T cells capable of regulating homeostasis. Our findings putatively implicate a role for dynamic physiologic cues generated within reactive SLO microenvironments that balance and modulate the transition to effector cells without exhausting naïve CD8$^+$ lymphocytes. We propose NADPH oxidase p47^{phox} and/or NADPH oxidase-mediated ROS is/are a regulator of these adaptive immune phenomenon. The mechanisms appear to involve the regulated suppression of prosurvival members of the Bcl-2 protein family that protect post-thymic naïve CD8$^+$ lymphocytes from Bim and Puma driven apoptosis as well as through mechanisms associated with the removal of *in vivo* suppressive factor(s) that allow enhanced apoptotic BH3-only protein expression *in vitro*. This indicates that the characterization of molecular pathways that are controlled by NADPH oxidase p47^{phox} and/or NADPH oxidase-mediated ROS may discern previously unrecognized targets for the development of immunomodulatory therapies.

Materials and Methods

Mice. p47^{phox}-deficient mice have been described.[13] Congenic p47$^{phox-/-}$ mice are on a C57BL/6NTac background. WT control mice (C57BL/6NTac) were obtained from Taconic Farms (Hudson, NY). Animal care was provided in accordance with Institutional Animal Care and Use Committee procedures approved by NIAID/NIH. NADPH oxidase-deficient mice were housed in aseptic conditions. Tissues showing gross evidence of infection were discarded and not used for the investigations reported.

Cell isolation. Lymph node single cell suspensions were prepared from peripheral mouse LNs or thymus. CD4$^+$ and CD8$^+$ T cells were negatively selected using the Dynal bead mouse CD4- or CD8-negative isolation kit (Invitrogen Corp., Carlsbad, CA) according to the manufacturer's protocol. The purity of each cell population was $>98\%$ as determined by flow cytometry.

Cell culture and stimulation. Lymph node purified CD4 or CD8 T lymphocytes were cultured at a concentration of 1×10^6 cell/ml in IMDM complete : IMDM (Gibco/Invitrogen Corp.) containing 10% FBS (Hyclone Laboratories, Logan, UT), 2.0 mM L-glutamine (Hyclone), 50 μM β-mercaptoethanol (β-ME, Sigma Aldrich, St. Louis, MO) and 100 U/ml penicillin and 10 U/ml streptomycin (Gibco/Invitrogen Corp.) supplemented with 10 U/ml rhIL-2 (Rohmann-LaRoche Inc., Nutley, NJ) or 100 ng/ml IL-7 (PeproTech, Rocky Hill, NJ). For initial experiments, cells were cultured using 10 – 100 U/ml rhIL-2. There was no difference in the relative cell viability differences between WT and p47$^{phox-/-}$ cells using 100 U/ml of IL-2. Subsequently for later experiments, the cells were cultured using 10 U/ml IL-2.

Caspase inhibition. Lymph node purified CD8$^+$ T cells were cultured in IMDM complete and supplemented with 10 U/ml rhIL-2 or 100 ng/ml IL-7, and treated with 50 μM Z-VAD (OMe)-FMK (EMD Chemicals, San Diego, CA).

Cell counts and viability. Resting CD4$^+$ or CD8$^+$ LN cells were incubated with IL-2 or IL-7 as indicated, and cell count and viability were determined. Viable and nonviable lymphocytes from cultures were differentially stained with DNA-binding dyes and the absolute number of viable *versus* nonviable nucleated cells were quantitated on the basis of cell size and staining properties using the Guava ViaCount (Guava Technologies, Hayward, CA) assay. Cells were diluted with the Guava Viacount (Guava Technologies) reagent in a total volume of 400 μl at the indicated time intervals. Cell counts and viable and dead cell numbers were determined using Guava ViaCount Software on the Guava PCA (Guava Technologies).

Antibodies, immunofluorescent staining and flow cytometry. Fluorescein isothiocyanate (FITC)-conjugated monoclonal antibodies (mAB) against CD11b (Mac-1), Gr-1, B220, CD44, CD25 and (BD Pharmingen,); R-phycoerythrin (PE)-conjugated mAB against B220, CD27, CD62L, CD69 and CD127 (IL-7R; BD Pharmingen); allophycocyanin (APC)-conjugated CD11b, CD3, CD4 and CD8 were used. Cells were stained with the designated FITC (1 : 250), APC (1 : 250) or PE (1 : 500)-conjugated mAb or isotype control for 25 min at room temperature in 1 – 2% FBS – HBSS containing purified rat antimouse CD16/CD32 Fc Block (BD Pharmingen) to minimize nonspecific binding. For the analysis, all cells were resuspended in 1 – 2% FBS – HBSS containing propidium iodide (50 ng/ml; Invitrogen) to distinguish viable cells. Cell acquisition was performed on the Becton Dickinson FACSort or FACSCalibur (BD Biosciences, San Jose, CA) using CellQuest Pro software (BD Biosciences). Analysis was performed using FlowJo software (FlowJo, LCC, Ashland, OR).

Adoptive transfer. Single cell suspensions were made from LNs from p47$^{phox-/-}$ mice (CD45.2 Thy 1.2) and Thy1.1$^+$ WT C57/BL6 mice. Ten million of each were injected i.v. into CD45.1 WT C57/BL6 recipients. LNs and spleen were harvested from recipients at 24 h and stained for surface markers CD45.1 PE, Thy.1 PerCp, CD44 FITC (BD Pharmingen), CD4 Pacific Blue, CD8 Alexa Flour 700, CD45.2 Alexa Flour 750 and Thy1.2 Pe-Cy5 (eBioscience, San Diego, CA). Cells were gated on CD45.2$^+$ CD45.1$^-$, and then analyzed for CD4, CD8 and CD44 staining among WT (Thy1.1$^+$ and Thy1.2$^-$) or KO (Thy1.2$^+$ and Thy1.1$^-$) donors. Cell acquisition was performed on the Becton Dickinson LSR II (BD Biosciences) using CellQuest Pro software (BD Biosciences). Analysis was performed using FlowJo software (FlowJo, LCC, Ashland, OR).

BrdU stimulation. p47$^{phox-/-}$ and WT mice were fed with BrdU (BD Pharmingen) in their drinking water at a concentration of 1 mg/ml for 5 days. LNs were harvested on day 5. Whole LN cell populations were stained with anti-CD4, CD8, CD44, B220 and BrdU antibodies (BD Pharmingen). Cell acquisition was performed on the Becton Dickinson LSRII (BD Biosciences) using CellQuest Pro software (BD Biosciences). Analysis was performed using FlowJo software (FlowJo, LCC, Ashland, OR).

Bcl-2 and Bax staining. Cells were washed twice in 1% FBS/PBS and surface stained for CD8 (1 : 500) and CD44 (1 : 125 – 500) as indicated. Cells were fixed according to the (Cytofix/Cytoperm Plus Kit, BD Pharmingen) manufacturer's protocol. Cells were stained for intracellular Bcl-2 (BD Pharmingen) or Bax (Santa Cruz, Santa Cruz, CA) according to the manufacturer's protocol. Conformational change in the Bax protein was assessed by intracellular immunostaining using a specific antibody that recognizes only the proapoptotic conformation : anti-Bax (6A7; BD Pharmingen) using the method described by Gómez-Benito *et al*.[29] Briefly, cells were cultured with IL-2 supplemented medium for 3 h. Then, 1×10^6 cells were fixed with 0.5% paraformaldehyde in PBS for15 min at 4°C and incubated for 25 min at room temperature with 0.5 μg of anti-Bax or a mouse IgG isotype control (BD Pharmingen) in 100 μl of PBS containing 0.1% saponin and 5% goat serum. Cells were washed with 0.03% saponin in PBS and incubated with a FITC-labeled antimouse IgG antibody (BD Pharmingen) at room temperature. Cell acquisition was performed on the Becton Dickinson FACSCalibur (BD Biosciences) using CellQuest Pro software (BD Biosciences). Analysis was performed using FlowJo software (FlowJo, LCC, Ashland, OR).

Cytochrome C release. Quantitative analysis of cytochrome C release from mitochondria was assessed by a modification of the method described by Waterhouse and Trapani.[29,30] Briefly, cells were cultured with IL-2 supplemented medium for 3 h. Then, 1×10^6 cells were permeabilized with 100 μl of digitonin (50 μg/ml in PBS containing 100 mM KCl) for 5 min on ice, fixed in 4% paraformaldehyde in PBS for 20 min at room temperature, and resuspended in 3% bovine serum albumin, 0.05% saponin in PBS (blocking buffer). Cells were incubated overnight at 4°C with a 1 : 500 dilution of anti-cytochrome C antibody (InnoCyte™ Flow Cytometric Cytochrome C Release Kit, Calbiochem, EMD Chemicals, Inc., Gibbstown, NJ) in blocking buffer, washed, and then incubated with a 1 : 300 dilution of FITC-labeled anti-mouse IgG antibody (InnoCyte™ Flow Cytometric Cytochrome C Release Kit, Calbiochem). Control cells were stained with a 1 : 300 dilution of the FITC-labeled anti-mouse IgG antibody in the absence of a primary antibody. Cell acquisition was performed on the Becton Dickinson FACSCalibur (BD Biosciences) using CellQuest Pro software (BD Biosciences). Analysis was performed using FlowJo software (FlowJo).

Cell death analysis. Lymph node purified CD8$^+$ T cells were cultured as indicated. Cells were harvested at the designated time, washed with 1%FBS/PBS and stained for surface CD8 and CD44 (BD Pharmingen). Mitochondrial membrane integrity and cell death were determined using the Mitoprobe kit (Invitrogen) or the Annexin V: PE Apoptosis Detection Kit I (BD Pharmalgen) according to the manufactures protocols.

Glucose oxidase stimulation. Lymph node purified CD8$^+$ T cells were cultured in IMDM complete without β-ME and supplemented with 10 U/ml rhIL-2 or 100 ng/ml IL-7. Cells were treated with the following range of GO (Sigma-Aldrich): log 10 concentration, 10 ng/ml – 1 pg/ml and log2 concentrations, 0.3 – 1.2 pg/ml. Cells counts were determined at 24 h using Guava ViaCount Software on the Guava PCA (Guava Technologies).

Cell fractionation and Western blot analysis. After CD8 isolation, cells were counted and resuspended at 1×10^6 cells/ml in IMDM complete with 10 U/ml rhIL-2 (Rohmann-LaRoche Inc.) for 1.5 h, and then washed with cold PBS. Cells were lysed in ice-cold mammalian protein extraction reagent (Pierce Biotechnology, Rockford IL), 1X mammalian protease inhibitor (Sigma-Aldrich) and 5 mM EDTA followed by sonication for 10 min. Insoluble material was removed by centrifugation at 12 000 $\times$ *g* at 4°C for 10 min. Equivalent amounts of protein were denatured in Laemmli buffer for direct resolution by 10–20% SDS-polyacrylamide gel electrophoresis (SDS-PAGE), and transferred to a nitrocellulose membrane (Millipore Corporation, Billerica, MA). Immunoblotting was performed using anti-Puma Ab, anti-Bim Ab, anti-BMF Ab, (Cell Signaling Technology, Danvers, MA), anti-Mcl-1 Ab, (Abcam Inc., Cambridge, MA) anti-actin Ab (Sigma-Aldrich), HRP-conjugated antirabbit Ab and HRP-conjugated antimouse Ab (GE Healthcare, Piscataway, NJ). Immunoreactive proteins were visualized using an ECL detection kit (GE Healthcare) upon exposure to BioMax™ light film (Kodak). For the relative quantification of the proteins, scanned images were analyzed using Image J.[33]

Statistical analysis. Means and S.E.M. of cell count and viability were determined. Differences between the group means were analyzed by the Student's *t*-test. (Prism 4, GraphPad Software Inc. San Diego, CA).

Acknowledgements. We thank Kevin Gardner and Richard Youle for helpful discussions and critique of an earlier draft of this manuscript. We also thank Harry

Malech and Michael Davis for careful review of this manuscript. This research was supported by the Division of Intramural Research of the National Institutes of Health/ National Institute of Allergy and Infectious Diseases.

1. Rathmell JC, Thompson CB. Pathways of apoptosis in lymphocyte development, homeostasis, and disease. *Cell* 2002; **109** (Suppl): S97–S107.
2. Guimond M, Fry TJ, Mackall CL. Cytokine signals in T-cell homeostasis. *J Immunother* 2005; **28**: 289–294.
3. Van Parijs L, Abbas AK. Homeostasis and self-tolerance in the immune system: turning lymphocytes off. *Science (New York, NY)* 1998; **280**: 243–248.
4. Walker LS, Abbas AK. The enemy within: keeping self-reactive T cells at bay in the periphery. *Nat Rev* 2002; **2**: 11–19.
5. Marrack P, Bender J, Hildeman D, Jordan M, Mitchell T, Murakami M *et al.* Homeostasis of alpha beta TCR+ T cells. *Nat Immunol* 2000; **1**: 107–111.
6. Marrack P, Kappler J. Control of T cell viability. *Annu Rev Immunol* 2004; **22**: 765–787.
7. Babior BM. The respiratory burst oxidase. *Adv Enzymol Relat Areas Mol Biol* 1992; **65**: 49–95.
8. Nauseef WM. Assembly of the phagocyte NADPH oxidase. *Histochem Cell Biol* 2004; **122**: 277–291.
9. Sauer H, Wartenberg M, Hescheler J. Reactive oxygen species as intracellular messengers during cell growth and differentiation. *Cell Physiol Biochem* 2001; **11**: 173–186.
10. Jackson SH, Devadas S, Kwon J, Pinto LA, Williams MS. T cells express a phagocyte-type NADPH oxidase that is activated after T cell receptor stimulation. *Nat Immunol* 2004; **5**: 818–827.
11. Assari T. Chronic Granulomatous Disease; fundamental stages in our understanding of CGD. *Med Immunol (London, England)* 2006; **5**: 4.
12. Rosenzweig SD. Inflammatory Manifestations in Chronic Granulomatous Disease (CGD). *J Clin Immunol* 2008; **28** (Suppl 1): S67–S72.
13. Jackson SH, Gallin JI, Holland SM. The p47phox mouse knock-out model of chronic granulomatous disease. *J Exp Med* 1995; **182**: 751–758.
14. Hildeman DA. Regulation of T-cell apoptosis by reactive oxygen species. *Free Radic Biol Med* 2004; **36**: 1496–1504.
15. Hildeman DA, Mitchell T, Teague TK, Henson P, Day BJ, Kappler J *et al.* Reactive oxygen species regulate activation-induced T cell apoptosis. *Immunity* 1999; **10**: 735–744.
16. Hockenbery DM, Oltvai ZN, Yin XM, Milliman CL, Korsmeyer SJ. Bcl-2 functions in an antioxidant pathway to prevent apoptosis. *Cell* 1993; **75**: 241–251.
17. Vella A, Teague TK, Ihle J, Kappler J, Marrack P. Interleukin 4 (IL-4) or IL-7 prevents the death of resting T cells: stat6 is probably not required for the effect of IL-4. *J Exp Med* 1997; **186**: 325–330.
18. Tan JT, Dudl E, LeRoy E, Murray R, Sprent J, Weinberg KI *et al.* IL-7 is critical for homeostatic proliferation and survival of naive T cells. *Proc Natl Acad Sci USA* 2001; **98**: 8732–8737.
19. Ku CC, Murakami M, Sakamoto A, Kappler J, Marrack P. Control of homeostasis of CD8+ memory T cells by opposing cytokines. *Science (New York, NY)* 2000; **288**: 675–678.
20. Fry TJ, Mackall CL. The many faces of IL-7: from lymphopoiesis to peripheral T cell maintenance. *J Immunol* 2005; **174**: 6571–6576.
21. Kishimoto H, Sprent J. Strong TCR ligation without costimulation causes rapid onset of Fas-dependent apoptosis of naive murine CD4+ T cells. *J Immunol* 1999; **163**: 1817–1826.
22. Jiang Q, Li WQ, Aiello FB, Mazzucchelli R, Asefa B, Khaled AR *et al.* Cell biology of IL-7, a key lymphotrophin. *Cytokine Growth Factor Rev* 2005; **16**: 513–533.
23. Bentley R. Glucose oxidase. In: Boyer PD, Lardy H, Myrbäck K (eds). *The Enzymes*, 2nd edn. Vol. 7, Academic Press: New York, 1963, pp 567–586.
24. Pazur JH. Glucose oxidase. In: Cowolick SP, Kaplan NO (eds). *Methods in Enzymology*, Vol. 9, Academic Press: New York, 1966, pp 82–87.
25. Kovanen PE, Leonard WJ. Cytokines and immunodeficiency diseases: critical roles of the gamma(c)-dependent cytokines interleukins 2, 4, 7, 9, 15, and 21, and their signaling pathways. *Immunol Rev* 2004; **202**: 67–83.
26. Park JH, Yu Q, Erman B, Appelbaum JS, Montoya-Durango D, Grimes HL *et al.* Suppression of IL7Ralpha transcription by IL-7 and other prosurvival cytokines: a novel mechanism for maximizing IL-7-dependent T cell survival. *Immunity* 2004; **21**: 289–302.
27. Spierings D, McStay G, Saleh M, Bender C, Chipuk J, Maurer U *et al.* Connected to death: the (unexpurgated) mitochondrial pathway of apoptosis. *Science (New York, NY)* 2005; **310**: 66–67.
28. Green DR, Kroemer G. The pathophysiology of mitochondrial cell death. *Science (New York, NY)* 2004; **305**: 626–629.
29. Gomez-Benito M, Marzo I, Anel A, Naval J. Farnesyltransferase inhibitor BMS-214662 induces apoptosis in myeloma cells through PUMA up-regulation, Bax and Bak activation, and Mcl-1 elimination. *Mol Pharmacol* 2005; **67**: 1991–1998.
30. Waterhouse NJ, Trapani JA. A new quantitative assay for cytochrome c release in apoptotic cells. *Cell Death Differ* 2003; **10**: 853–855.
31. Youle RJ, Strasser A. The BCL-2 protein family: opposing activities that mediate cell death. *Nat Rev Mol Cell Biol* 2008; **9**: 47–59.
32. Antunes F, Cadenas E, Brunk UT. Apoptosis induced by exposure to a low steady-state concentration of H2O2 is a consequence of lysosomal rupture. *Biochem J* 2001; **356** (Pt 2): 549–555.
33. Rasband WS. ImageJ, US National Institutes of Health: Bethesda, Maryland, USA, http://rsb.info.nih.gov/ij/, 1997–2007.

Supplementary Information accompanies the paper on Cell Death and Differentiation website (http://www.nature.com/cdd)